IJST (2013) 37A2: 189-197
Iranian Journal of Science & Technology
http://www.shirazu.ac.ir/en

Stable isotopes geochemistry of the bauxite horizons in the Dehdasht area, southwest Iran

A. Zarasvandi*, A. Foroughinia, H. Pourkaseb and A. Charchi

Department of Geology, Shahid Chamran University (SCU), Ahvaz, Iran
E-mail: Zarasvandi_a@scu.ac.ir

Abstract

The karst-bauxite deposits of the Dehdasht region in the southwest of Iran, are situated unconformably between Cenomanian and Santonian shallow marine limestones. The white, gray, black, pisolitic, red and yellow bauxites are the main horizons in these deposits from bottom to top. In this study, the combinations of oxygen, hydrogen, carbon and sulfur isotopes of the main bauxite units were utilized to trace bauxitization processes, climatic and environmental conditions. The $\delta^{18}O$ and δD values of boehmite and kaolinite minerals, not only suggest a likely inheritance relation between them, but also suggests no remarkable climate changes during occurrence of bauxite horizons in Cretaceous. The $\delta^{18}O$ values of about -7 ‰ and -8 ‰ inferred for the waters at the time of kaolinite crystallization and achieved kaolinization paleo-temperature more than 30˚C, represent low paleo-latitude location of the study area during the Cretaceous. The negative $\delta^{13}C$ values from the carbonate matrix of bauxite-bearing minerals, as low as -25 ‰, indicate carbon derivation from the biodegradation of organic matter under aerobic and anaerobic conditions. The positive $\delta^{34}S$ values of pyrites reveale sulfate-limiting condition during diagenesis that is consistent with biological fractionation of sulfur in a closed system by sulfate-reducing bacteria.

Keywords: Bauxite; stable isotope; climate; sulfate-reducing bacteria; Dehdasht; Iran

1. Introduction

Global warming is one of the most considerable features in the Earth's climate history during middle-Cretaceous [1]. These climatic conditions allowed the intensive karst and bauxite development in the middle-Cretaceous [2]. Bauxites record various information about climatic, biological and pedogenic conditions of the paleo-environments and hence are the best key indicators for climate reconstruction [3].

The Stable isotope geochemistry have been widely used for the bauxite genesis and reconstruction of paleo-temperature [4]. H_2O bearing minerals are considered as one of the main factors that control isotopic composition of bauxite deposits [5]. Therefore these minerals can be used as paleo-thermometers of the water system at the time such minerals were formed [6]. The oxygen isotope composition of weathered minerals is useful for delineating weathering prosesses and paleoclimate during their formation [7]. Hydrogen isotope ratios may be modified by post-formational isotopic exchange with meteoric water at surfical temperature or diagenetic condition in higher temperatures [8]. The geochemical characteristic of S and C isotopes provide useful information about environmental conditions and biogeochemical processes that control formation of bauxite [9].

Zagros orogenic–metallogenic province in Iran hosts a number of important Cretaceous bauxite deposits [10]. The study area is located in the Dehdasht region, in the Zagros belt. The most important bauxite deposits in Dehdasht area are karst-related deposits. These bauxitic deposits are boehmite-type that developed along the contact between Sarvak and Ilam Formations from Cenomanian to Santonian. Bauxite sequence in the study area consists of white, gray, black, pisolitic, red and yellow bauxites [11]. The variation from gray to pisolitic horizons represents the transformation of minerals and redox stage in bauxite sequences [3]. Zarasvandi, et al. [11] studied the geochemistry, mineralogy and genesis of the bauxite deposits in Zagros, but there is no published study about the stable isotopes geochemistry of the bauxite deposits.

The present study investigate the $\delta^{18}O$ and δD content of kaolinite and boehmite in gray and pisolitic horizons, due to their usefulness as a tracer for bauxitization processes and paleoclimatic changes [12]. Also, in this work carbon and sulfur isotope compositions were used to investigate the role of different processes during the deposition of carbonate and sulfur minerals in bauxite horizons.

*Corresponding author
Received: 20 January 2013 / Accepted: 8 April 2013

2. Geological Setting

Three major tectonic elements with NW–SE trends are recognized in Iran due to collision of the Arabian continent and Iranian micro-continent. They include the Zagros Fold and Thrust belt (ZFTB), Sanandaj-Sirjan metamorphic zone (SSZ) and Urumieh-Dokhtar magmatic arc (UDMA) [13, 14]. The Zagros orogenic belt extends for almost 2000 km across Iran and Iraq, through Syria and southeastern Turkey [15, 14] (Fig. 1). The tectonic evolution of the Zagros can be summarized as a series of Late Proterozoic, Permian and Mesozoic rift events that were followed by closure of Neo-Tethys in the Early to Middle Eocene [14].

The carbonates and detrital sedimentary rocks (about 12 km) are the dominant rocks in Zagros [10]. The Dehdasht bauxite deposits are located 40 km northeast of Dehdasht city in the Zagros fold belt (Fig. 1). The Cretaceous sedimentary succession in the study area includes the Bangestan Group (Sarvak, Surgah, Ilam, Gurpi, Pabdeh, and Asmari Formations), which is dominated by widespread cliff-forming shallow-marine limestones. Faults with N–S and E–W trends cut the Bangestan Group [11]. The Sarvak Formation of the Bangestan Group (Albian–Santonian) was deposited during Cenomanian to Early Turonian time. These carbonates were affected by a major unconformity (Turonian) that created extensive erosion surfaces and karstification. Karstic bauxite deposits are the best indicators of subaerial exposure and karstification of the Upper Sarvak Formation [16].

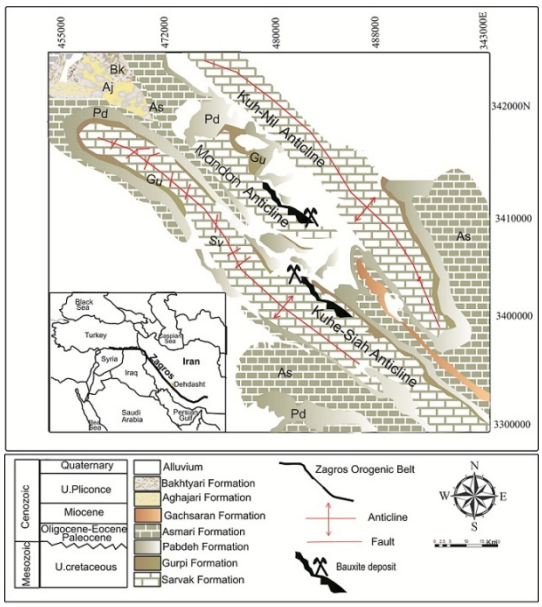

Fig. 1. Generalized geographical and geological map of the study area

The study area consists of a series of compact anticlines and synclines. Generally, the anticlines are composed of a series of uplifted blocks separated by numerous faults, these features preserve old land surfaces in small down-faulted blocks [10]. The Mandan, Kuh-e-Siah and Kuh-e-Nil anticlines are exposed in the study area and the karstification of the Sarvak Formation in these anticlines is very typical. The studied deposits are situated in the southern limb of the Mandan anticline and northern limb of the Kuh-e-Siah anticline (Fig. 1). These deposits are located along the disconformity surface between the shallow-marine neritic limestones of the Sarvak and Ilam Formations (Fig. 2). The studied bauxite horizons commonly consist of white, gray, black, pisolitic, red and yellow bauxites, from bottom to top. The bottom of these bauxites deposits is made up of Sarvak argillites (or argillaceous limestone) (Fig. 2). Uplift in Oligocene-Miocene time with erosion exposed the bauxite horizon to its present configuration.

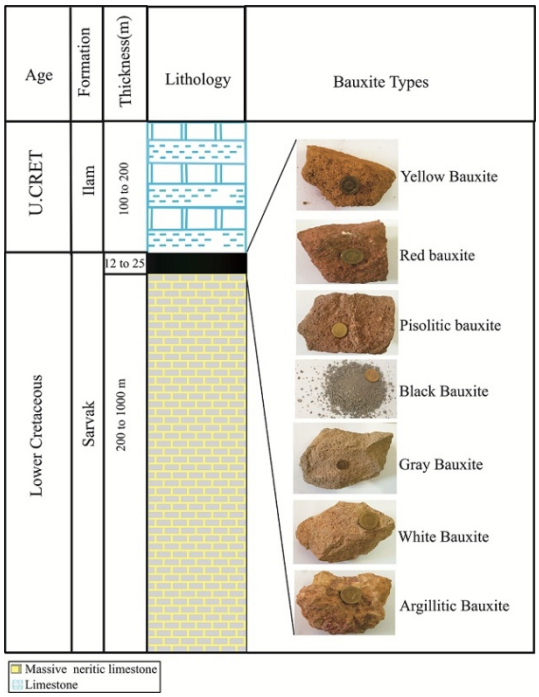

Fig. 2. General geological profile of the bauxite horizons at study area

3. Sampling and Analytical Methods

The samples from the six bauxite horizons in the study area were selected for stable isotope analysis (Table 1). The samples were crushed with mortar and pestle, then sieved and the mineral separates were made by hand picking based on mineralogical studies. Mineralogy and estimating the relative abundances of each sample was determined by X-ray Diffraction (XRD) at the Isotope Laboratory of

Queen's University, Kingston, Canada. Pure monomineralic separates of kaolinite matrix and boehmite (separated from pisolites) in the gray and pisolitic horizons were selected for oxygen and hydrogen isotopes analysis. Isotope measurements were performed using a Finnigan MAT 252 mass spectrometer. Oxygen isotope compositions were measured using the BrF_5 method [17]. Hydrogen isotope compositions of these minerals were determined using the methods of Kyser and O'Neil [18]. All values are reported using the δ notation in units of per mil relative to V-SMOW. The $\delta^{18}O$ analyses were reproducible to ±0.2 ‰ and δD values were reproducible to ±3 ‰. Carbonate $\delta^{13}C$ values were measured on CO_2 released from a dissolution of 0.5 -1.5 mg of sample in H_3PO_4, using a Thermofiningan Gas Bench II. Carbon isotopic composition was reported in standard δ notation in units of per mil relative to the Vienna Peedee Belemnite standard. The $\delta^{13}C$ values were reproducible to ±0.2 ‰. For sulfur analysis, SO_2 was produced from 3 to 10 mg of sulfide minerals loaded into tin capsules and reacted with CuO at 1,400°C in a Hestream using the thermal conversion/elemental analyzer-isotope ratio mass spectrometer technique. The analytical uncertainty for $\delta^{34}S$ is 0.5 ‰. Sulfur data are reported in the delta notation relative to Canyon Diablo Triolite.

Table 1. Mineralogical Characteristics of the analyzed bauxite samples

Bauxite	Macroscopic characteristics
Pisolitic	Red-brown and white red-brown and white, rusty-red weathering laterite. well-rounded clasts of very fine gravel size occur in a red matrix containing clay and iron oxide.
Gray	Mottled gray, dusty-yellow brown weathering laterite. Well-rounded clasts of very fine gravel to very coarse sand size occur in a light gray matrix containing clay. Fine grains of dark gold pyrite occur in clusters and are dispersed throughout the rock.

4. Results

4. 1. X-ray diffraction (XRD)

The XRD spectra for pisolitic and gray horizons are shown in Fig. 3. The pisolitic horizon mainly consists of kaolinite with a significant, but less abundance of diaspore, hematite, boehmite and minor anatase, while XRD spectra for gray horizon indicate that boehmite is the dominant mineral. It is mainly associated with kaolinite, diaspore, pyrite and minor amount of anatase (Table 2 and Fig. 3).

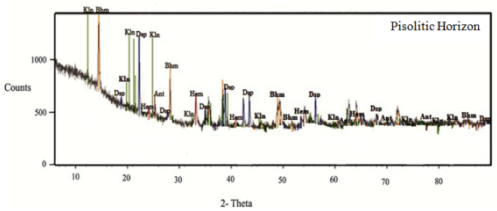

Fig. 3. XRD patterns of pisolitic and gray bauxites (Dsp= diaspore, Hem= hematite, Kln= kaolinite, Ant= anatase, Py= pyrite, Bhm= Boehmite

4. 2. Isotope study

The Kaolinites from the matrix of pisolitic horizon exhibit $\delta^{18}O$ and δD values in a range of 13.9 ‰ to 15.5 ‰ and -71 ‰ to -76 ‰, respectively. The measured values of $\delta^{18}O$ and δD for kaolinites from the matrix of gray horizon range from 15 ‰ to 16.6 ‰ and -67 ‰ to -72 ‰ respectively (Table 2 and Fig. 4). In a similar point, boehmite $\delta^{18}O$ and δD values of pisolites of pisolitic horizon vary within the narrow range of 8.6 ‰ to 10.7 ‰ and, -65 ‰ to -78 ‰, respectively. The boehmite samples from pisolites of gray horizon exhibit very consistent $\delta^{18}O$ and δD values, ranging from 9.6 ‰ to 10.2 ‰ and -71 ‰ to -78 ‰, respectively (Table 2 and Fig. 4). The kaolinites of matrix are plotted away from the 30°C kaolinite line ($\delta D = 7.55\ \delta^{18}O - 219$) from Savin and Epstein [19] and the boehmite of pisolites are plotted close to the boehmite line ($\delta D = 7.84\ \delta^{18}O - 114.2$) of Bird et al. [20] (Fig. 5). The carbon isotope composition of the carbonate matrix of pisolitic and gray horizons is -26.22 ‰ Peedee belemnite (PDB) and -26.199 ‰ (PDB), respectively. Calcite cements in the pisolites of pisolitic and gray horizons display $\delta^{13}C$ values -26.35 ‰ (PDB) and -26.303 ‰ (PDB), respectively (Table 3 and Fig. 6). The sulfur isotope compositions of pyrites from the gray bauxite show a range from 7.2 ‰ to 14 ‰ (Table 3). Considering the data set as a whole, homogenous isotopic composition of the kaolinites and boehmites can be observed, which indicates a relatively constant isotopic condition during the development of bauxite horizons. Also, similar $\delta^{13}C/^{12}C$ depletion-values in these horizons suggest that similar processes participated in calcites formation.

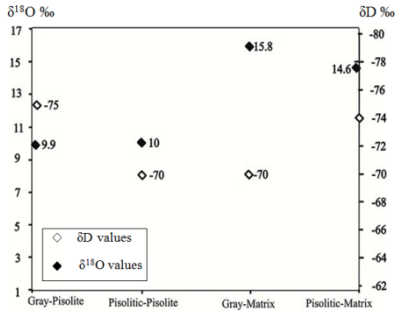

Fig. 4. Average of isotopic values of the boehmite and kaolinite from the bauxite horizons of the Dehdasht area

Table 2. quantitative mineralogical analyses and results of oxygen and hydrogen isotopic analyses of bauxite horizons of the Dehdasht area

Horizon	Mineralogy (%)	$\delta^{18}O$ matrix (‰)	δD matrix (‰)	$\delta^{18}O$ pisolite (‰)	δD pisolite (‰)
Pisolitic	Kln Bhm Dsp Hem Ant	13.9	-76	8.6	-78
	62 12 22 13 1	14	-76	9.9	-74
		14.4	-75	10	-70
		14.6	-74	10.1	-69
		14.7	-74	10.1	-69
		15	-73	10.2	-68
		15.2	-73	10.4	-67
		15.5	-71	10.7	-65
Average		14.6	-74	10	-70
Gray	Kln Bhm Dsp Py Ant	15	-72	9.6	-78
	17 52 16 10 4	15.3	-71	9.7	-77
		15.3	-71	9.8	-76
		15.8	-70	9.9	-75
		16	-70	9.9	-75
		16.2	-69	10	-74
		16.2	-69	10	-74
		16.6	-67	10.2	-71
Average		15.8	-69.9	9.9	-75

All $\delta^{18}O$ and δD values are reported relative to SMOW.
Bhm=Boehmite, Kln=Kaolinite, Dsp=Diaspore, Hem=Hematite, Ant=Anatase, Py=Pyrite

Table 3. Carbon and Sulfur isotopic value of calcites and pyrite from the Dehdasht area

	$\delta^{13}C/^{12}C$ (matrix)	$\delta^{13}C/^{12}C$ (pisolite)	$^{34}\delta$
Horizon	VPDB (‰)	VPDB (‰)	S_{CDT} (‰)
Pisolitic	-26.222	-26.35	-
Gray	-26.199	-26.303	7.2
			8.6
			10.3
			14

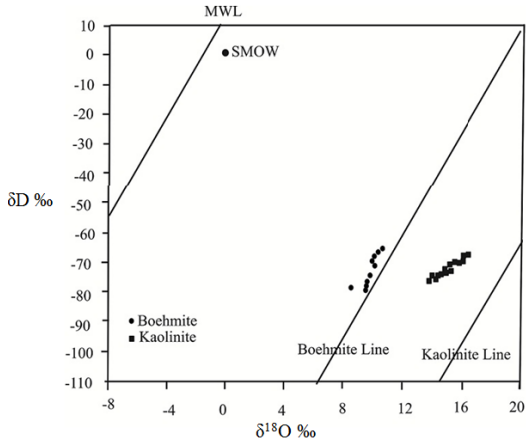

Fig. 5. Isotope composition of the boehmite and kaolinite from the pisolitic and gray horizons. The kaolinite line from Savin and Epstein [19]; boehmite line from Bird et al. [20]. (MWL=Meteoric Water line of Craig [21]; SMOW= Standard Mean Ocean Water)

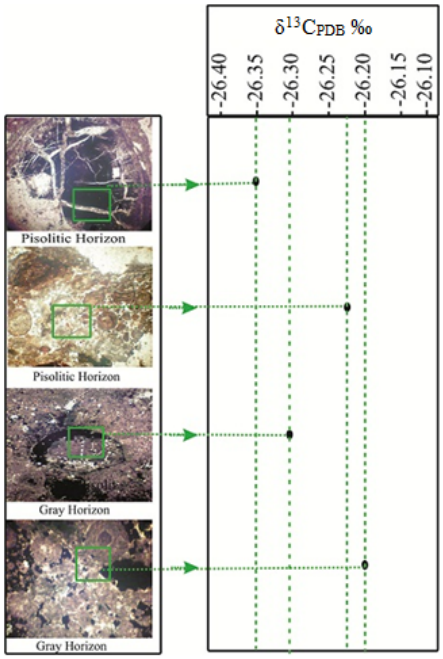

Fig. 6. Carbon isotopic value of carbonate components of the bauxite horizons in the study area

5. Discussion

5. 1. Mineralogical composition

Based on the prevailing iron types, bauxite deposits are classified as ferrous and ferric bauxites [22]. The Dehdasht bauxite horizons can be categorized into ferric bauxite with hematite as the main iron phase (pisolitic horizon) and ferrous bauxite with pyrite as the main iron mineral (gray horizon). The Kaolinite is considered as common clay mineral in bauxite deposits and may be residual, and can be formed by syngenetic or epigenetic processes [23]. The kaolinite-rich horizons (Table 2) and coexistence of kaolinite with diaspore and boehmite suggest that kaolinite probably formed by epigenetic replacement of alumina in boehmite by dissolved silica. This process also causes boehmitization and diasporization [24, 23]. Epigenetic kaolinite occupies fracture-filling or micro-cracks which represent circulation of SiO_2-rich solutions by cracks during epigenetic process [25]. When silica content of water is much higher than 2.5 x 10^{-5} mole/liter, low-pH solutions are able to silicificate the boehmite and form the kaolinite [26].

Özlü [27] suggested that diaspore can be formed as syngenetic, syndiagenetic and epigenetic. In the ore samples, aggregates of euhedral crystals of diaspore fill voids of the pisolitic horizon that indicate leaching of iron [28] during the epigenetic stage. Also, the presence of diaspore in veinlets coexisting with secondary calcite suggest diaspore have formed during the epigenetic stage [27].

The gray horizon is characterized by the occurrence of pyrite, this indicates microbial activity under the euxinic conditions during bauxite diagentic stage [28]. The presence of boehmite and hematite in the pisolitic horizon reveal the acidic-oxidant condition [29]. The minor amounts of anatase (Table 2) are a sign of reduction and low pH conditions during formation of the bauxite horizons. With respect to the presence of hematite, boehmite, diaspore and pyrite minerals, it can be stated that the depositional-diagenetic environment of bauxite horizons is probably vadose to phreatic [30]. Considering the above, due to contributing diagenetic and epigenetic processes during the formation of bauxite horizons, mineralogical composition represents multistage process [22].

5. 2. Isotope signatures

Carbonates dissolution due to meteoric diagenesis creates a feature called karst. Karstification also can occur in the other diagenetic environments such as deep burial and mixing zones [16]. As mentioned, the bauxitization in the study area occurred along the disconformity surface between the shallow-marine neritic limestones of the Sarvak and Ilam Formations (Fig. 2). In an isotopic study of the upper Sarvak limestones from southwestern Iran, Hajikazemi et al. [16] reported $\delta^{13}C$ and $\delta^{18}O$ values of the carbonate matrix, calcite cements and calcitic rudist shells. The $\delta^{18}O$ of a carbonate is associated with the $\delta^{18}O$ composition and temperature of the water from which it precipitated. Depleted $\delta^{18}O$ values of Sarvak limestones (as low as -10 ‰) show diagenetic alteration in the Sarvak limestones occurred in the presence of meteoric water or under shallow burial (decreasing salinity and increasing temperatures) conditions [31]. Depleted $\delta^{13}C$ values such as -3.5 ‰ supports the notion that Sarvak limestone has experienced post-depositional isotope exchange with meteoric waters during karstification process [16]. The karstification provides spaces for bauxite deposition [11]. Considering variation in oxygen isotope compositions of Sarvak limestones it can be shown that climate was an important factor in bauxite formation in the study area.

5. 3. Carbon Isotopes: An Index of Microbial Activity

The carbon isotopic values for the matrix and pisolites of pisolitic and gray horizons are given in Table 3. The data indicate similar source for the carbon in horizons. According to Pisciotto and Mahoney [32], the depletion of carbonate $\delta^{13}C$ values (as low as –25 ‰) indicate carbon derivation from the oxidation of organic matter under aerobic and anaerobic conditions. Organic matter decay in sediments at shallow burial by assemblages of bacteria cause formation of ^{12}C enriched CO_2 [4]. The low values of $\delta^{13}C$ (-26 ‰) in the study area samples are probably related to the oxidation of organic matter during carbonates diagenetic process.

The carbon isotope values of the samples represent the importance of organic matter and microbial activity during mineralization. Decay of organic matter in anaerobic environment is considered to be a reason for the occurrence of pyrite [33, 25, 28]. However, both biotic and abiotic reactions are able to form pyrite during the bauxitization processes [34]. Two forms of pyrite crystals have been observed in the gray bauxite; euhedral and framboidal. These two types of pyrites morphology are also reported in the Upper Sarvak Formation [16]. Formation of pyrites in bauxite deposits have been described elsewhere such as Greece, China and the Taurides, Turkey [35, 36, 9]. During the pyrite oxidation process, due to production of H^+, PH of pore-water decreases and hence dissolution of carbonate phases is enhanced

by the reaction shown below [37]:

$4CaCO3 + 4H^{+} \longrightarrow 4Ca^{2+} + 4HCO^{3-}$

As is CO_2 produced by degradation of organic carbon in aerobic condition, alkalinity will increase and settling of Ca-Mg-carbonates in these conditions will cause Ca^{2+} and Mg^{2+} absorption on the surface of bacteria [3]. Therefore, carbonate $\delta^{13}C$ values of pisolitic horizon indicate calcite derivation from abundant light-carbon CO_2 in aerobic microbial oxidation processes.

5. 4. Sulfur Isotopes

The $\delta^{34}S$ values of sedimentary sulfides have been used as a tracer to evaluate the sulfate reduction and for reconstruction of paleo-environments [38]. Sulfur isotopes data for the Doğankuzu bauxite deposits show that pyrite has low $\delta^{34}S$ values, supporting their formation in an euxinic environment. Positive $\delta^{34}S$ values of pyrites from the gray bauxite of the study area (Table 3) indicate that shallow-marine or brackish-water environments likely were involved in pyrites formation [9]. The occurrence of sulfate reduction in an open or closed system is an important factor that controls the sulfur isotope variations of natural sulfides [4]. The sulfur isotope compositions of samples indicate $\delta^{34}S$ enrichment consistent with biological fractionation of sulfur in a closed system by sulfate-reducing bacteria [39].

Although sulfur isotope data of more pyrites in the study area are not available, early diagenetic fromboidal pyrites observed by microscopic studies may bring the conclusion that increase in sulfur isotopes values can be probable and the later generation of pyrites in a closed system would not be unexpected [38]. Within such scenario bacterial sulfate reduction occurred under sulfate-limiting conditions and caused shifting to the more positive $\delta^{34}S$ values [40].

Partial replacement of fracture-filling calcite cement with pyrite in matrix (Fig. 6) indicates its occurrence during the last stages of diagenesis. Occurrence of pyrite and ferrous calcites in some samples is one advantage of an anaerobic environment [41]. Thus it seems that calcitic cements and veins may be formed during mid-diagenesis or in the first stage of uplift during later diagenesis. These iron-bearing cements and veins occurred as a result of CO_2-release under reduction conditions. Some of the calcitic veins may also be influenced by meteoric water. These calcites have no Fe [42]. The fracture-filling forms of calcite observed in the horizons of the study area reveal the effects of tectonic deformation.

5. 5. Oxygen and Hydrogen isotopes

According to Bird and Chivas [43], the $\delta^{18}O$ values of kaolinites decrease with time. Fig. 7 represents the trend of Australian kaolinites through time. In this diagram Tertiary samples fall closest to the line, while the Permian samples are the most discordant. Movement toward the left of the kaolinite line indicates the evolution of lower oxygen isotope compositions. Kaolinites of pisolitic and gray horizons of the study area have $\delta^{18}O$ values between 13.9 ‰ to 15.5 ‰ and 15 ‰ to 16.6 ‰, respectively, that fall in the field of Cretaceous Australian bauxite deposits. Moreover, the results show that the kaolinite samples of the study area are situated between the kaolinite line and the Supergene/hypogene line (S/H) of Sheppard and Gilg [44], indicating the equilibration of kaolinites with meteoric waters and supports the non-hydrothermal origin for kaolinites.

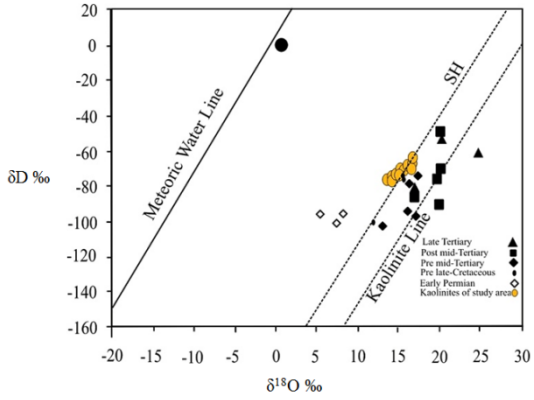

Fig. 7. Stable isotope composition of clay minerals from Australian regolith profiles (Data from Bird and Chivas [43] and Kaolinites from the study area. M.W.L=meteoric water line; SMOW= Standard Mean Ocean Water; S/H=supergen/hypogene kaolinite line of Sheppard and Gilg [44]; K.L=Kaolinite line of Savin and Epstein [19]

The $\delta^{18}O$ and δD isotope values of the boehmites and kaolinites (Table 2 and Fig. 4) represent the uniform isotopic composition in the studied horizons that indicate the relatively constant isotopic condition [6] and simple history of bauxites formation. Isotopic comparison between the boehmite and kaolinite (Fig. 5) not only suggest a likely inheritance relationship between them [45], but also suggests no remarkable climate changes during occurrence of cretaceous bauxite horizons. Kaolinite samples are plotted to the left of the kaolinite line (Fig. 5). As the most likely explanation, it can be stated that the kaolinites have formed in the stage of boehmite resilicification [43]. According to Dangić [23, 24] and Mameli et al. [25], percolation of SiO_2-rich solutions and the consequent silicification process will cause the instability of boehmite. Hence, oxygen from boehmite structure may enter into the structure of

the neo-formed kaolinites and shift the kaolinite $\delta^{18}O$ values leftward of the kaolinite line [43]. Kaolinization is concomitant with Al remobilization [23, 24], therefore boehmite samples close to the boehmite line (Fig. 5) indicate secondary boehmites formed by remobilization of Al from solution [45]. The boehmite of the gray horizon has lower δD and $\delta^{18}O$ values (Table 2), which reveals equilibrium with lighter waters isotopically. It is suggested that monsoon climate prevailed in the area during the bauxitization process [20].

The $\delta^{18}O$ and δD values of clay minerals reflect the temperatures and isotopic composition of the waters from which they crystallized [46]. Fig. 8 illustrates the average values of $\delta^{18}O$ and δD for kaolinites of pisolitic and gray horizons so that ancient waters have W_1 and W_2 composition during their formations. W_1 and W_2 values represent $\delta^{18}O$ values of about -7 ‰ and -8 ‰ for kaolinites formation. With respect to the above approaches, 1000 $\ln^{O}\alpha$ K−w is about 23. Using Sheppard and Gilg equation [44]: 1000 $\ln^{O}\alpha$ K−w = 2.76 * $10^6/T_2$ -6.75 (T in K), the resulted kaolinization paleo-temperatures will be more than 30˚C, which suggest low-latitude position for study area during Cretaceous [47]. In the rainy season, light isotopes of oxygen and hydrogen are in abundance and $\delta^{18}O$ and δD values are depleted, while in a dry season the two latter values are abundant. At low-latitudes, seasonal variations in $\delta^{18}O$ and δD values of precipitation reveal seasonal variation in the amount/intensity of precipitation [7]. The obtained $\delta^{18}O$ values of the ancient waters (Fig. 8) can be considered in accordance with rainfall and the warm, wet climatic conditions [47].

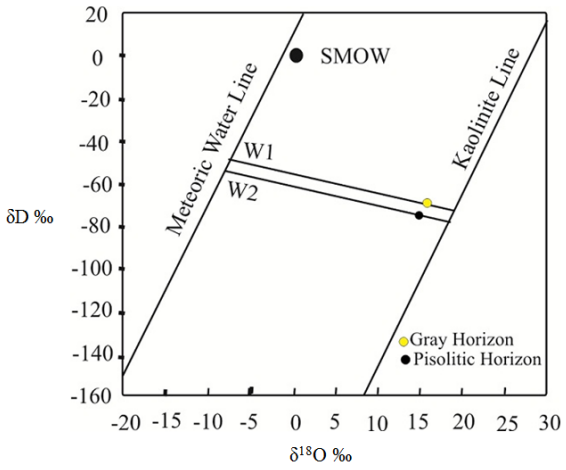

Fig. 8. Plot of δD vs. $\delta^{18}O$ average values for kaolinites of pisolitic and gray horizons. The kaolinite line is from Savin and Epstein [19]. The $\delta^{18}O$ value about -7 ‰ and -8 ‰ inferred for the ancient waters (W_1 and W_2) respectively, at the time of kaolinites formation

The obtained temperatures reflect the surface micro-environmental conditions [6]. These temperatures are consistent with the results of Hajikazemi et al. [16] who inferred middle Cretaceous temperatures of 25˚C and 36˚C from the oxygen isotope compositions of calcite in the Sarvak Formation in southwestern Iran.

6. Conclusion

This study was an attempt to evaluate the stable isotope compositions of minerals in pisolitic and gray horizons to investigate environmental conditions which led to the changes of bauxite type during their formations. Stable isotopes data from the Dehdasht bauxite horizons of Iran lead to the following:

1. The results of quantitatively mineralogical studies of these bauxite horizons revealed diagenetic and epigenetic processes changed the early composition of minerals. Moreover, it indicates that depositional/diagenetic environment of the horizons is vadose to phreatic.
2. The constant hydrogen and oxygen isotopic data from kaolinite and boehmite indicate the probable inheritance between them. Samples of kaolinite are plotted between the boehmite and the kaolinite lines. This behavior may be related to the kaolinite formation by resilicification of boehmite. Boehmite samples plotted close to the boehmite line indicate remobilization of Al from solution (secondary boehmite).
3. The $\delta^{18}O$ values of about -7 ‰ and –8 ‰ inferred for the ancient waters at the time of kaolinites crystallization and achieved paleo-temperature more than 30˚C were consistent with rainfall during the summer monsoon.
4. The $\delta^{13}C$ carbonate values of the carbonate matrix and calcite cements in the pisolits of pisolitic and gray horizons are as low as –25 ‰. This approach represents the oxidation of organic matter through microbial reduction of sulfate and aerobic microbial oxidation during diagenetic process of carbonates.
5. With increasing burial depth during mid-diagenes or in the first stage of uplift during later diagenes, CO_2 released from organic decay has formed calcite, therefore the uplift derived fractures may be filled by calcite (reduction condition) and some of them may influenced by meteoric diagenesis, which are non -iron calcites.
6. Sulfur isotopic compositions clearly indicate this sulfur is derived from bacterial sulfate reduction under sulfate-limiting conditions that caused ^{34}S isotope enrichment.

Acknowledgments

This work was supported by a grant in 2012 from the vice-chancellor for Research and Technology of Shahid Chamran University. The authors would like to thank Kurt Kyser for stable isotope analyses at the Queen's University, Canada.

References

[1] Fluteau, F., Ramstein, G., Besse, J., Guiraud, R. & Masse, J. P. (2007). Impacts of palaeogeography and sea level changes on Mid-Cretaceous climate. *Palaeogeography, Palaeoclimatology, Palaeoecology*, *247*, 357-381.

[2] Simone, L., Bravi, S., Carannante, G., Masucc, I. & Pomoni-Papaioannou, F. (2012). Arid versus wet climatic evidence in the "middle Cretaceous" calcareous successions of the Southern Apennines (Italy). *Cretaceous Research*. In Press.

[3] Hao, X., Leung, K., Wang, R., Sun, W. & Li, Y. (2010). The geomicrobiology of bauxite deposits. *Geoscience Frontiers*, *1*, 181-89.

[4] Hoefs, J. (2009). *Stable Isotope Geochemistry*. Sixth ed. Springer-Verlag Berlin Heidelberg, 285pp.

[5] Chivas, A. R. & Bird, M. I. (1995). Palaeoclimate from Gondwana clays. *In*: Churchmann, G. J., Fitzpatrick, R. W & Eggleton, R. A. (eds), Clays: Controlling the Environment. *Proceeding of the 10th International Clay Conference*. Adelaide, Australia. CSIRO Pub, Melbourne, 333-338.

[6] Horbe, A. M. C. (2011). Oxygen and hydrogen isotopes in pedogenic minerals- Implications for paleoclimate evolution in Amazonia during the Cenozoic. *Geoderma*, *163*, 178-184.

[7] Girard, J. P., Freyssinet, P. & Chazotu, G. (2000). Unraveling climatic changes from intraprofile variation in oxygen and hydrogen isotopic composition of goethite and kaolinite in laterites: An integrated study from Yaou, French Guiana. *Geochimica et Cosmochimica Acta*, *64*, 409-426.

[8] Bird, M. I. & Chivas, A. R. (1989). Stable-isotope geochronology of the Australian regolith. *Geochimica et Cosmochimica Acta*, *53*, 3239-3256.

[9] Öztürk, H., Hein, J. R. & Hanilci, N. (2002). Genesis of the Dog˘ankuzu and Mortas¸ Bauxite Deposits, Taurides, Turkey: Separation of Al, Fe, and Mn and Implications for Passive Margin Metallogeny. *Economic Geology*, *97*, 1063-1077.

[10] Zarasvandi, A., Charchi, A., Karranza, E. J. M. & Alizadeh, B. (2008). Karst bauxite deposits in the Zagros Mountain Belt, Iran. *Ore Geology Reviews*, *34*, 521-53.

[11] Zarasvandi, A., Carranza, E. J. M. & Salamab Ellahi, S. (2012). Geological, Geochemical and Mineralogycal characteristics of the Mandan and Deh-Now bauxite deposites, Zagros Fold Belt, Iran. *Ore Geology Reviews*, *48*, 125-138.

[12] Girard, J. P., Freyssinet, P. & Morillon, A. C. (2002). Oxygen isotope study of Cayenne duricrust paleosurfaces: implications for past climate and laterization processes over French Guiana. *Chemical Geology*, *191*, 329-343.

[13] Alavi, M. (1994). Tectonics of the Zagros orogenic belt of Iran: new data and interpretations. *Tectonophysics*, *229*, 211-238.

[14] Alavi, M. (2004). Regional stratigraphy of the Zagros fold-thrust belt of Iran and its proforeland evolution. *American Journal of Science*, *304*, 1-20.

[15] Vera, J. D., Gines, J., Oehlers, M., Mcclay, K. & Doski, J. (2009). Structure of the Zagros fold and thrust belt in the Kurdistan Region, northern Iraq. Trabajos de Geología, *Universidad de Oviedo*, *29*, 213-217.

[16] Hajikazemi, E., Al-Aasm, I. S. & Coniglio, M. (2010). Subaerial exposure and meteoric diagenesis of the cenomanian-Turonian Upper Sarvak Formation, southwestern Iran. *Geological Society of London, 330*, 253-272.

[17] Clayton, R. N & Mayeda, T. K. (1963). The use of bromine pentafluoride in the extraction of oxygen from oxides and silicates for isotopic analysis. *Geochim Cosmochim Acta*, *27*, 43-52.

[18] Kyser, K. & O'Neil, J. (1984). Hydrogen isotope systematic of submarine basalts. *Geochim Cosmochim Acta*, *48*, 48-53.

[19] Savin, S. M. & Epstein, S. (1970). The oxygen and hydrogen isotope geochemistry of clay minerals. Geochimica et Cosmochimica Acta, 34, 25-42.

[20] Bird, M. I., Chivas, A. R. & Andrew, A. S. (1989). A stable-isotope study of lateritic bauxites. *Geochimica et Cosmochimica Acta*, *53*, 1411-1420.

[21] Craig, H. (1961). Isotopic variations in meteoric waters. *Scienc*e, *133*, 1702-1703.

[22] Laskou, M. (2005). Pyrite-rich bauxite from the Parnassos-Ghiona zone, Greece. In: Mao et al. (eds), 8th SGA Meeting, "*Mineral Deposits Research Meeting the Global Challenge*" Beijing, 1007-1010.

[23] Dangić, A. (1985). Kaolinization of bauxite: A study in the Vlasenica bauxite area Yugoslavia I. alteration of matrix. *Clays and Clay minerals*, *33*, 517-524.

[24] Dangić, A. (1988). Kaolinization of bauxite: A study of the Vlasenica bauxite area Yugoslavia II. Alteration of oolites. *Clays and Clay minerals, 36*, 439-447.

[25] Mameli, P., Mongelli, G., Oggiano, G. & Dinelli, E. (2007). Geological, geochemical and mineralogical features of some bauxite deposits from Nurra (Western Sardinia, Italy): insights on conditions of formation and parental affinity. *Int J Earth Sci* (*Geologische Rundschau)*, *96*, 887-902.

[26] Oggiano, G. & Mameli, P. (2001). The bauxite of North-Western Sardinia, *Rendiconti della Facoltà di Scienze MM.FF.NN. dell Università di Cagliari, 71*, 59-73.

[27] Özlü, N. (1985). New facts on diaspore genesis in the AksekiSeydisehir bauxite deposit (Western Taurus, Turkey): *Travaux du ICSOBA*, *14-15*, 53-62.

[28] Kalaitzidis, S., Siavalas, G., Skarpelis, N., Araujo, C. V. & Christanis, K. (2010). Late Cretaceous coal overlying Karstic bauxite deposits in the Parnassus-Ghiona unit, Central Greece: coal characteristics and depositional environment. *International Journal of Coal Geology*, *81*, 211-226.

[29] Amini, L., Shamanian, G. H., Raghimi, M. & Jafarzadeh, R. (2011). Mineralogycal, geochemical and genetical investigations of the Jajarm karst bauxite deposite,NE Iran. *Iranian journal of crystallography and mineralogy*, *19*, 413-426.

[30] Liu, X., Wang, Q., Deng, J., Zhang, Q., Sun, S. & Meng, J. (2010). Mineralogical and geochemical investigations of the Dajia Salento-type bauxite deposits, western Guangxi, China. *Journal of Geochemical Exploration, 105*, 137-152.

[31] Nagarajan, R., Sial, A. N., Armstrong-Altrin, J. S., Madhavaraju, J. & Nagendra, R. (2008). Carbon and oxygen isotope geochemistry of Neoproterozoic limestones of the Shahabad Formation, Bhima basin, Karnataka, southern India. *Revista Mexicana de Ciencias Geológicas*, *25*, 225-235.

[32] Pisciotto, K. A. & Mahoney, J. J. (1981). Isotopic survey of Diagenetic carbonates deep sea drilling project, leg63. *In* Yeats, R. S. & Haq, B.U et al. (eds), *Init. Repts. DSDP* Washington (U.S. Govt. Printing Office), *63*, 595-609.

[33] Laskou, M. & Economou-Eliopoulos, M. (2007). The role of microorganisms on the mineralogical and geochemical characteristics of the Parnassos-Ghiona bauxite deposits, Greece. *Journal of Geochemical Exploration*, 93, 67-77.

[34] Karadağ, M. M., Küpeli, S., Aryk, f., Ayhan, A., Zedef, V. & Döyn, A. (2009). Rare earth element (REE) geochemistry and genetic implications of the Mortas- bauxite deposit (Seydis-ehir/Konya-SouthernTurkey). *Chemie der Erde*, *69*, 143-159.

[35] Laskou, M., Economou-Eliopoulos, M. & Mitsis, I. (2010). Bauxite ore as an energy source for bacteria driving iron-leaching and bio-mineralization. *Hellenic Journal of Geosciences*, *45,* 163-173.

[36] Yuefei, Z., Rucheng, W., Jianjun, L. & Yillang, L. (2006). Ferruginous Microspherules in Bauxite at Maochang, Guizhou Province, China: Products of Microbe-Pyrite Interaction? *Acta geologica sinica, 80*, 604-609.

[37] Pirlet, H., Wehrmann, L. M., Brunner, B. A., Frank, N., Dewanckel, J., Roolj, D. V., Foubert, A., Swennen, R., Naudts, L., Boone, M., Cnudde, V. & Henriet, J. P. (2010). Diagenetic formation of gypsum and dolomite in a cold-water coral mound in the Porcupine Seabight, off Ireland. *Sedimentology*, *57*, 786-805.

[38] Strauss, H. & Schieber, J. (1990). A sulphur isotope study of pyrite genesis: The Mid-Proterozoic Newland formation, Belt Supergroup, Montana. *Geochimica et Cosmochimica Acta 54*, 197-204.

[39] Wacey, D., Wright, D. T. & Boyce, A. J. (2007). A stable isotope study of microbial dolomite formation in the Coorong Region, South Australia. *Chemical Geology*, *244*, 155-174.

[40] Strauss, H. (2003). Sulphur isotopes and the early Archaean sulphur cycle. *Precambrian Research 126*, 349-361.

[41] Odigi, M. I. & Amajor, L. C. (2008). Origin of carbonate cements in Cretaceous sandstunes from lower Benue Trough, Nigeria: evidence from petrography and stable isotope composition. *Scientia Africana*, *7*, 123-139.

[42] Mahboubi, A., Moussavi-Harami, R., Mahmoudi-Gharaee., M. H., Mansouri Daneshvar, P. & Khaneabad, M. (2009). Paragenetic sequenceinterpretation of Upper Cretaceous carbonates of northeast of Bajestan. Journal of Science,University of Tehran, *34*, 75-85.

[43] Bird, M. I. & Chivas, A. R. (1989). Stable-isotope geochronology of the Australian regolith. *Geochimica et Cosmochimica Acta*, *53*, 3239-3256.

[44] Sheppard, S. M. F. & Gilg, H. A. (1996). Stable isotope geochemistry of clay minerals. *Clay mineral*, *31*, 1-24.

[45] Vitali, F., Longstaffe, F. J., Bird, M. I., Gage, K. L. & Caldwell, W. J. E. (2001). Hydrogen-isotope fractionation in aluminum hydroxides: Synthesis products versus natural samples from bauxites. *Geochimica et Cosmochimica Acta*, *65*, 1391-1398.

[46] Gilg, H. A. (2000). D-H evidence for the timing of kaolinization in Northeast Bavaria, Germany. *Chemical Geology*, *170*, 5-18.

[47] Feng, W. & Yapp, C. J. (2009). $^{18}O/^{16}O$ and D/H ratios of pedogenic kaolinite in a North American Cenomanian laterite: Paleoclimatic implications. *Geochimica et Cosmochimica Acta*, *73*, 6249-6263.